Nanoscale

Accepted Manuscript

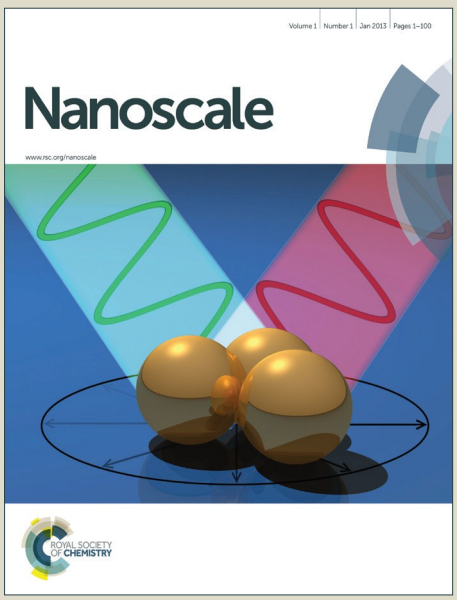

ROYAL SOCIETY OF CHEMISTRY

www.rsc.org/nanoscale

Nanoscale

RSCPublishing

ARTICLE

Cite this: DOI: 10.1039/x0xx00000x

Substrate-Bound Growth of Au-Pd Diblock Nanowire and Hybrid Nanorod-plate

Received 00th January 2015,
Accepted 00th January 2015

DOI: 10.1039/x0xx00000x

www.rsc.org/

Jiating He,[†] Yawen Wang,[†] Zhanxi Fan,[‡] Zhenhui Lam,[†,§] Hua Zhang,[‡] Bin Liu,[§] and Hongyu Chen[*,†]

We expand the scope of the previously developed Active Surface Growth mode for growing substrate-bound ultrathin Pd (d = 4 nm) and Ag nanowires (d = 30 nm) in aqueous solution under ambient conditions. Using Au nanorods as the seeds, selective growth at the contact line between the rod and the substrate eventually leads to an attached Pd nanoplate. The unique growth mode also allows sequential growth of different materials via a single seed, giving substrate-bound Au-Pd diblock nanowires. The new abilities to use seed shape to pre-define the active sites and to apply sequential growth open windows for new pathways to hybrid nanostructures.

Introduction

Advance of synthetic capability is the main thrust in nano-science and nanotechnology. As single-component nanostructures have been extensively studied, the field starts to move towards increasingly sophisticated nanostructures. Hybrid nanostructures have become a hot topic in the recent literature. The ability to precisely join different materials together at the nanoscale opens a window to exploit their synergistic effects, which have shown great promises in catalysis,[1-4] nanoelectronics,[5-7] and biomedical applications.[8-10] In comparison to the large number of reports on hybrid nanoparticles (NPs),[1,7,11] the synthesis of hybrid nanowires (NWs) is not well developed.[2,12-17]

Among the hybrid motifs, block NWs are generally more difficult than core-shell NWs (Figure 1), whose synthesis involves the simple overcoating of a material on a NW. For synthesizing block NWs, the ends of the pre-synthesized NWs must be selectively activated against the side surfaces for the deposition of the growth materials.

The challenge in creating hybrid segments in a NW is to grow different materials while maintaining the one-dimensional (1D) growth mode: (1) In vapor-liquid-solid (VLS) growth, the molten seed ensures unidirectional and sequential growth of the NW. Thus, diblock NW can be prepared if the materials have epitaxial interface and are both compatible with the growth method.[18-20] (2) In templated growth, typically the template ensures the 1D growth mode. Thus, vapor phase or electrochemical deposition can force sequential material deposition, with few requirements on the hybrid interface.[21,22] Other than these two methods, this approach cannot be easily realized because the competitive homogeneous nucleation (the growth outside the template) is difficult to avoid when filling the nanoscale cavities in a template. (3) A few cases of hybrid pentagonal NWs are known, where the five-fold twinning is essential in restricting lateral growth and promoting the 1D growth mode.[23,24] To make block NWs, all segments must be compatible with the five-fold twinning, with epitaxial interface in between. Given the symmetrical ends of a NW, growing ABA-type triblock NW[2,14-16] is easier than AB-type diblock NW. (4) Several semiconductor NWs are known to maintain their intrinsic 1D growth mode, even when starting from the surface of a different nanocrystal. Depending on the number of matching facets on the seed, the facet-specific growth can lead to ABA-type triblock NWs or elongated tetrapods.[25]

Recently, we reported the facile preparation of substrate-bound ultrathin Au NWs,[26,27] where the highly specific growth at the Au-substrate interface opens a convenient route for the sequential growth of hybrid NW segments. In this report, we expanded the scope of this method by growing Pd and Ag NWs (Figure 2 and 3). Thus, sequential addition of reactants can easily lead to sophisticated hybrid nanostructures. Depending

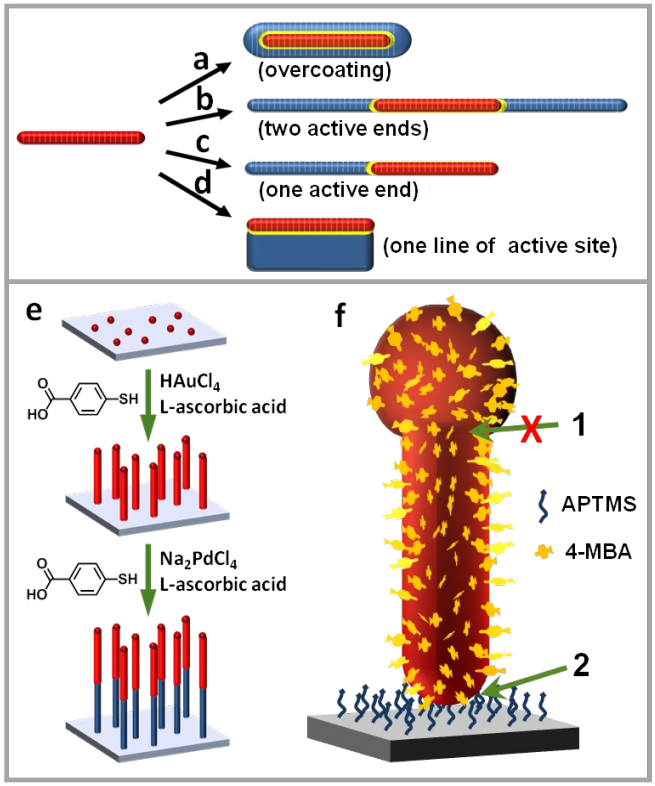

Figure 1. Schematics illustrating the growth of different kinds of hybrid nanostructures depending on the active sites (highlighted in yellow): (a) core-shell NWs, (b) ABA-type triblock NWs, (c) AB-type diblock NWs, and (d) hybrid nanoplates. (e) Schematics illustrating the growth of diblock NWs *via* the Active Surface Growth mode and (f) the ligand-governed selective growth; after the NW emerges, the active growth site remains at the ligand-deficient NW-substrate interface 2.

on the shape of the active sites, AB-type diblock Pd-Au NWs (Figure 4) and hybrid nanoplates (Figure 6) were synthesized.

In our previous study, we demonstrated the critical role of the strong ligand 4-mercaptobenzoic acid (4-MBA) in the Active Surface Growth, where the ligand inhibited deposition on all exposed seed surface except the seed-substrate interface.[26] Growth only occurred at this active site when the emerging nanocrystal was pushed up into a NW, whose exposed side surface was rapidly passivated by ligands. As such, the NW diameter was determined by the dynamic competition between the deposition of Au at the active site and the ligand inhibition at its boundary. With this understanding of the underlying mechanism, the growth mode is obviously independent of the specific properties of the metal. However, our initial trials of growing Ag and Pd NWs were all unsuccessful, leading to overcoating of the seed NPs with no sign of NWs. With different metal systems, the possible variables are the rates in reducing the metal salts and the affinity of the ligand to the metal ions and surfaces. Our general strategy is to screen the ligand concentration and to reduce the rate of metal deposition, so as to promote the Active Surface Growth mode and minimize the homogeneous nucleation in the solution.

Experimental section

Materials. Hydrogen tetrachloroaurate (III) ($HAuCl_4$, 99.9%, Au 49% on metals basis, Alfa Aesar), sodium chloropalladate(II) (Na_2PdCl_4, Alfa Aesar), silver nitrate ($AgNO_3$, Sigma Aldrich), 4-mercaptobenzoic acid (4-MBA, 90%, Sigma Aldrich), 3-aminopropyltrimethoxysilane (APTMS, Sigma Aldrich), sodium citrate tribasic dihydrate (99.0%, Sigma Aldrich), sodium borohydride ($NaBH_4$, Sigma Aldrich), L-ascorbic acid (Sigma Aldrich), hexadecyltrimethylammonium bromide (CTAB, Sigma Aldrich), ethanol (analytical grade) were used for preparing 4-MBA solution. Deionized water (resistance > 18.2 MΩ/cm) was used in all reactions. Copper specimen grids (300 mesh) with formvar/carbon support film were purchased from Beijing XXBR Technology Co.

Characterization. Transmission electron microscopy (TEM) images were collected on a JEM-1400 (JEOL) operated at 100 kV. Field emission scanning electron microscopy (SEM) images were collected on a JEOL JSM-6700F. High-resolution TEM (HRTEM) images were taken from JEOL 2100F field emission transmission electron microscopy, which is coupled with energy dispersive X-ray spectroscopy.

Preparation of TEM Samples. TEM grids were treated with oxygen plasma in a Harrick plasma cleaner/sterilizer for 45 s to improve the surface hydrophilicity. The hydrophilic face of the TEM grid was then placed in contact with the sample solution. A filter paper was used to wick off the excess solution on the TEM grid, which was then dried in air for 30 min.

Synthesis of citrate-stabilized Pd, Ag, and Au seeds (*d* = 3-5 nm). A 50 mL flask was filled with 0.2 mL sodium citrate (1 wt%) and 14 mL aqueous solution of H_2PdCl_4 (0.4 mM). Then 0.6 mL of ice-cold $NaBH_4$ solution (0.1 M) was added with vigorous stirring. The solution turned from brown to gray, indicating the formation of Pd NPs. To prepare Ag and Au seeds, $AgNO_3$ and $HAuCl_4$ were used as precursor, respectively; all other conditions were unchanged.

Synthesis of substrate-bound Pd NWs. A piece of Si wafer (about 1 cm^2) with thermal oxide layer was treated with O_2 plasma for 10 min to improve its surface hydrophilicity. The Si/silica wafer was then reacted with APTMS (5 mM) for 0.5 h to functionalize the surface with amino group. Subsequently, the wafer was soaked in excess citrate-stabilized Pd seeds solution for 0.5 h to ensure their adsorption. The seed-attached wafer was then rinsed with water and immersed in a water/ethanol (*v*/*v* = 1:2) solution of ligand 4-MBA (2.0 mM), Na_2PdCl_4 (2.4 mM) and L-ascorbic acid (4.3 mM). After a 30 min reaction, the wafer was washed using ethanol and dried in air.

For preparing Pd NWs using 3-5 or 15 nm[28] Au NPs as seeds, all reaction conditions were the same except that citrate-stabilized Au NPs with different diameter were used as the seeds.

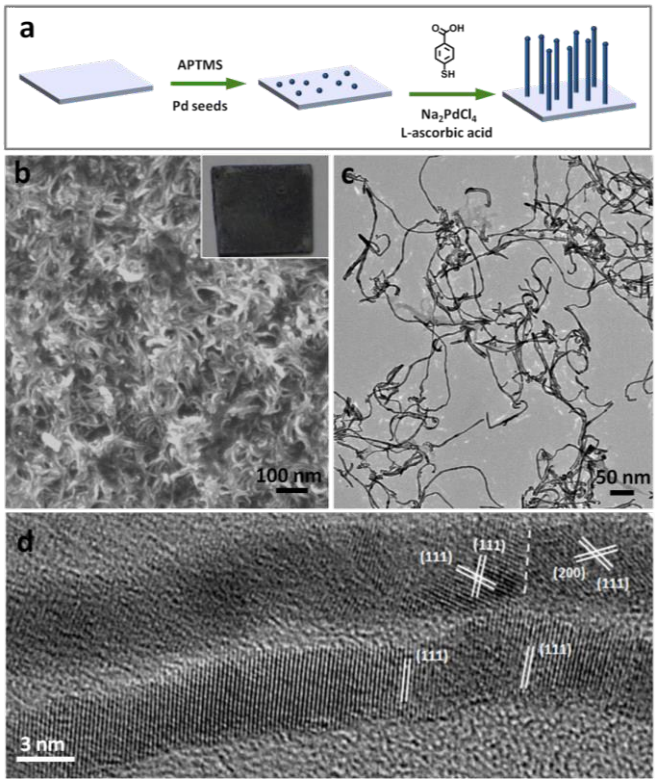

Figure 2. (a) Schematics illustrating the growth of substrate-bound Pd NWs. (b) SEM image of a dense layer of ultrathin Pd NWs grown on Si/silica wafer. The inset shows a photograph of the resulting Si/silica wafer (about 1 cm^2). (c) TEM image of the Pd NWs detached from the substrate by sonication. (d) HRTEM image of typical Pd NWs in (c). The white dash line shows a twin boundary in the NW.

Synthesis of substrate-bound Ag NWs. A Si/silica substrate (about 1 cm^2) functionalized with amino group was incubated with excess Ag seeds to adsorb a thin layer of seeds on its surface. Then, the substrate was soaked in a solution of 4-MBA (1.0 mM), $AgNO_3$ (1.5 mM) and then L-ascorbic acid (final 1.3 mM) was added drop wise into the solution at a rate of 120 μL/min. After the addition of the reductant, the wafer was rinsed with ethanol and dried in air.

Synthesis of substrate-bound diblock Au-Pd NWs. A Si/Silica substrate (about 1 cm^2) functionalized with amino group was incubated with Au seeds (d = 3-5 nm) solution for 0.5 h and then rinsed with water twice to remove the excess Au seeds. The seed-adsorbed wafer was then soaked in a water/ethanol (v/v = 1:2) solution containing 4-MBA (350 μM), $HAuCl_4$ (1.7 mM) and L-ascorbic acid (4.1 mM) for 20 s. The wafer attached with Au NWs was then rinsed with ethanol to remove the residue reagents and then immediately immersed in another reaction solution containing 4-MBA (2.0 mM), Na_2PdCl_4 (2.4 mM) and L-ascorbic acid (4.3 mM). After 30 min, the wafer was rinsed with ethanol and dried in air. The two growth steps can also be reversed to synthesize Pd-Au diblock NWs.

Synthesis of hybrid nanorod-plate. Au nanorods[29] were used as seeds for the growth of nanoplates. The as-synthesized nanorod solution was centrifuged twice for 8 min at 5200 g to remove the excess CTAB. A Si/Silica wafer (about 1 cm^2) functionalized with amino group was then incubated with the purified nanorod solution for 30 min and then it was blow-dried. Subsequently, the wafer was immersed in a reaction solution of 4-MBA (2.0 mM), Na_2PdCl_4 (2.4 mM) and L-ascorbic acid (4.3 mM). After 30 min, the wafer was wash by ethanol and dried in air for further characterization.

Results and Discussion

Pd NWs. Directly applying the conditions used for growing Au NWs did not work for Pd NWs. Considering the rapid growth of the nanowires (200 nm in 30 min), the packing of 4-MBA on the newly emerged Pd surface is likely not dense enough for inhibiting Pd deposition, leading to Pd overcoating on the seeds. However, if excess 4-MBA is used, it can totally inhibit the seed surface preventing NW growth. With careful study, the growth of ultrathin Pd NWs was achieved within a small window of the preparative conditions.

Specifically, Pd NPs of 3-5 nm in diameter were used as the seeds. They were adsorbed on a Si/silica wafer, which was then soaked in a reaction solution containing the ligand 4-MBA (2.0 mM), the Pd source Na_2PdCl_4 (2.4 mM) and the reducing agent L-ascorbic acid (4.3 mM). After 30 min, the wafer surface turned black, indicating successful metal deposition (Figure 2b, inset). Only the thin layer of solution right above the wafer turned grey, whereas the undisturbed solution elsewhere remained the orange color of the initial mixture (4-MBA with Na_2PdCl_4). This observation indicates that the reduction reaction can only occur near the seeds on the substrate. The wafer was then retrieved, rinsed with ethanol, and dried in air. As revealed by SEM, a dense layer of ultrathin Pd NWs fully covered the substrate surface (Figure 2b).

To isolate the Pd NWs for TEM characterization, they were detached from the substrate by sonication and the resulting solution was centrifuged. As shown in Figure 2c, the Pd NWs were not perfectly straight and they were about 4 nm in diameter and 200 nm in length. HRTEM showed that the typical Pd NWs were polycrystalline with twin defects (Figure 2d), similar to the Au NWs in our previous report.[26]

Slight modification of the above reaction conditions led to undesirable results. For example, increasing the 4-MBA concentration (from 2.0 to 2.3 mM) caused no growth of the seeds and no color change in the solution, indicating that the excess 4-MBA has totally inhibited the growth of the seeds.[30] On the other hand, decreasing the 4-MBA concentration (1.7 mM) caused insufficient inhibition of the Pd surface. As a result, homogeneous nucleation occurred in the solution, giving rise to colloidal Pd NPs and the outcompeted short NWs on the substrate.[30] These factors were the reason for our initial failures. While the NW growth can be achieved in the narrow range of [4-MBA] = 1.8-2.2 mM, the best concentration was 2.0 mM. Similarly, keeping the 4-MBA concentration at

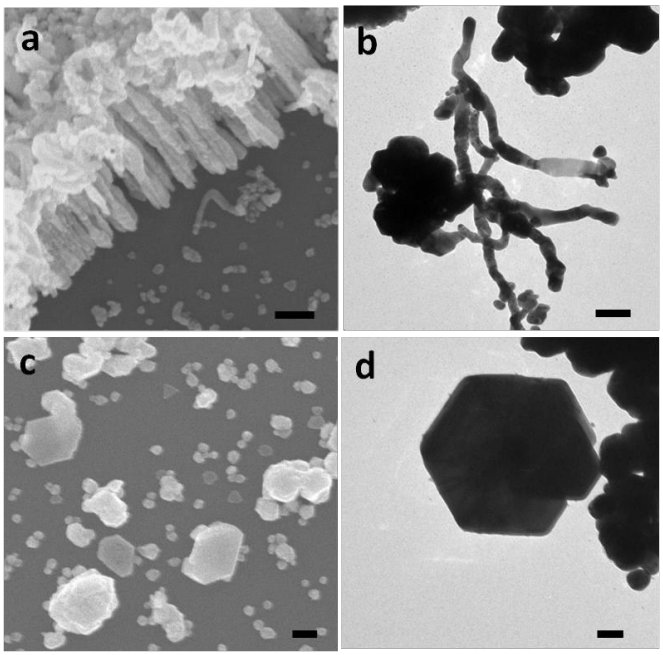

Figure 3. (a) SEM and (b) TEM images of the substrate-bound Ag NWs grown on Si/silica wafer using 1.0 mM 4-MBA. With small increase of ligand concentration (1.5 mM), only Ag nanoplates can be obtained: (c) SEM and (d) TEM images of the Ag plates. The TEM samples were detached from substrates by sonication. All scale bars = 100 nm.

constant but changing the rate of metal deposition (by changing the concentration of metal salt and reductant) showed that only a small range of conditions were suitable for the NW growth.[30]

Ag NWs. Substrate-bound Ag NWs can also be grown using the same method, but the reductant L-ascorbic acid has to be slowly introduced to slow down the rate of Ag reduction. Otherwise, the reaction between L-ascorbic acid and $AgNO_3$ would be too fast and the oversupply of Ag atoms would lead to homogeneous nucleation giving lots of colloidal Ag NPs. More specifically, the seed-adsorbed Si/silica wafer was immersed in a reaction solution of 4-MBA (1.0 mM), $AgNO_3$ (1.5 mM), to which L-ascorbic acid (final 1.3 mM) was added drop wise at a rate of about 0.6 μmol/min (120 μL/min).

As shown in Figure 3a,b, the resulting Ag NWs are less uniform in diameter than the Pd NWs. Some sections of the NWs appeared to be plate-like, likely due to the stability of the MBA-stabilized Ag facets. The width of the resulting Ag NWs (d = 16-38 nm, Figure 3a) is significantly larger than the ultrathin Pd and Au NWs.[26,27] Not all the seeds on the substrate were able to grow into NWs. Some seeds were grown into large clusters of nanoplates.[30] Increasing the ligand concentration (>1.0 mM) did not reduce the width of the NWs. Instead, Ag nanoplates were obtained with their faces parallel to the substrate. Apparently, the strong tendency in forming ligand-specific Ag facets (Figure 3c,d) disrupted the Active Surface Growth mode.

The growth of Pd and Ag NWs from substrate-bound seeds is consistent with the general characteristics of the Active

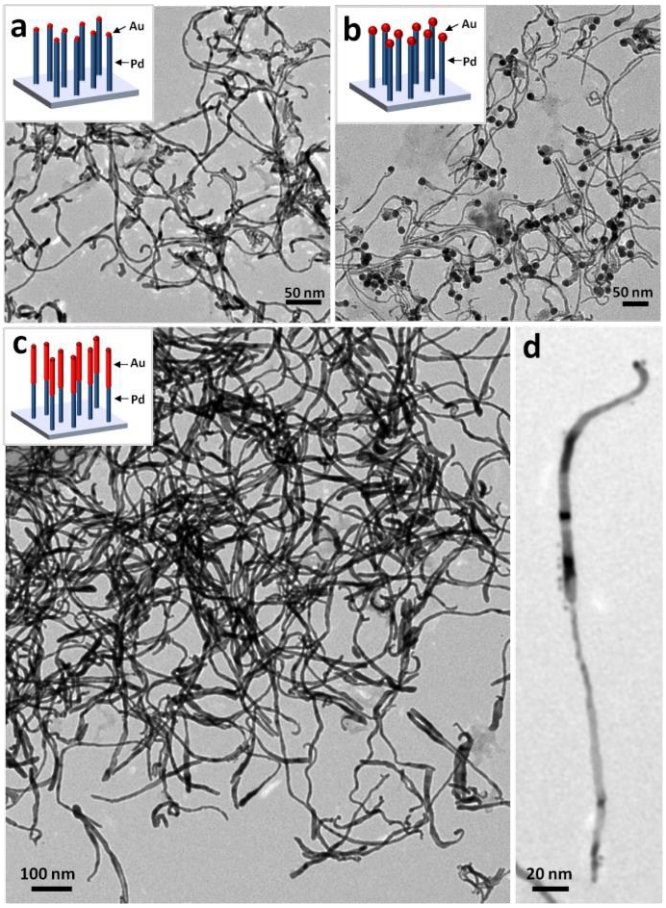

Figure 4. Schematics and TEM images of the substrate-bound ultrathin Pd NWs grown from (a) 3-5 nm and (b) 15 nm Au seeds; (c) ultrathin diblock Au-Pd NWs. (d) high-magnification TEM image of a typical diblock NW. The samples for TEM characterization were detached from substrates by sonication.

Surface Growth (Figure 1e,f), in terms of the selective growth at the NW-substrate interface and the dynamic control of the NW diameter. Our Ag NWs of about 30 nm in diameter are among the thinnest in the literature..[31-35] The dynamic ligand inhibition provides an effective means for restricting lateral growth, in comparison to the pentagonal Ag NWs, in which case the NWs have to be thick enough for the five-fold twinning defects to restrict the lateral growth.[24] Most importantly, our method is unique in providing a direct route to substrate-bound NWs, in comparison to the templated approaches where the template removal is often problematic. The method is also facile and can be readily applied to a large substrate surface with complex morphology.

Hybrid NWs. With these developments, the system provides a facile route to hybrid nanostructures. The easiest approach is to use NPs of different materials as seeds for growing NWs. For instance, using Au NPs (d = 3-5 nm) as seeds to grow Pd NWs (d = 4 nm), the morphologies of the emerging NWs are almost the same as that using Pd seeds (Figure 4a). Because of the same sizes of the seeds and NWs, the original seeds are difficult to distinguish after the growth.

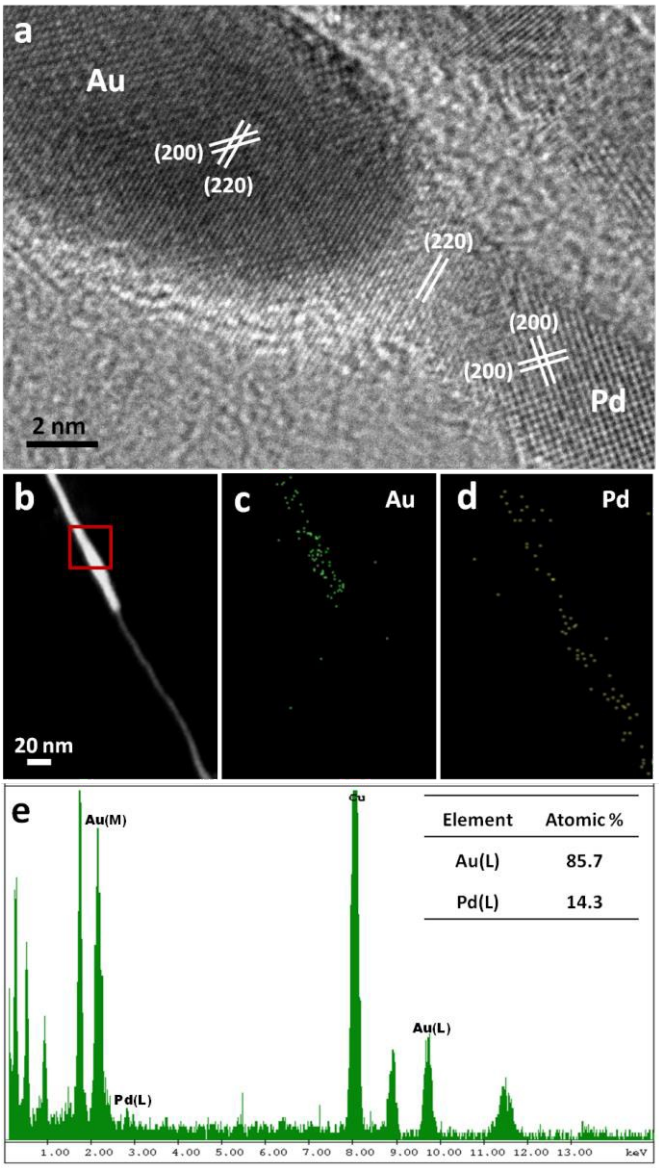

Figure 5. (a) Representative HRTEM image shows the epitaxial growth of Pd segment from the end of Au segment in a typical diblock NW. (b) Representative HAADF-STEM image and EDS mapping of (c) Au and (d) Pd. (e) EDS analyses of the section highlighted by the red square in (b).

When larger Au NPs (d = 15 nm) were employed as the seeds, as shown in Figure 4b, almost every thin Pd NW (about 4 nm) is bonded to a Au head at the end. The diameter of the spherical end was measured to be about 15 nm, suggesting that the seeds had barely grown except at the active site. The width of Pd NW segments is still 4 nm, which is unchanged given the same reactant concentrations. The fact that the NW width is independence of the seeds is consistent with the Active Surface Growth mode.[26]

Diblock NWs. Obviously, the most intriguing question is whether the NW growth would continue when a different growth material is used. For growing the first Au segment in diblock Au-Pd NWs, the seed-adsorbed Si/silica wafer was

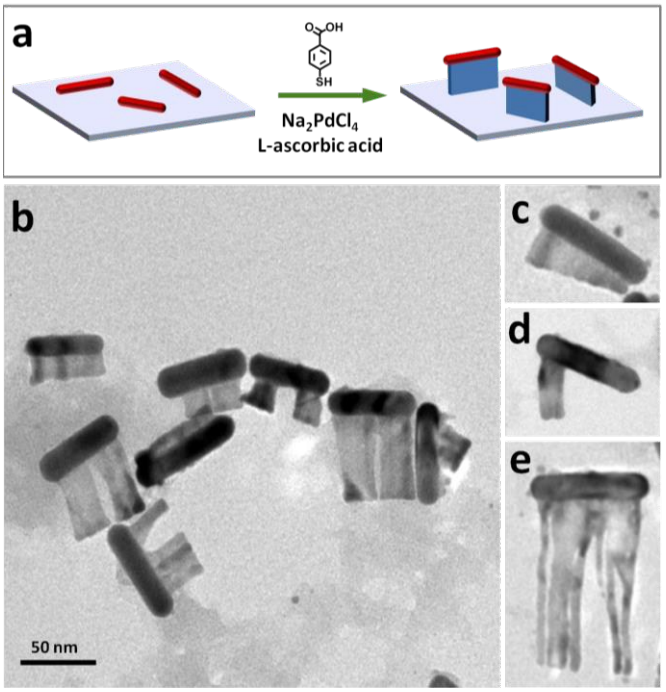

Figure 6. (a) Schematics illustrating the growth of Pd nanoplates from substrate-adsorbed Au nanorods. (b-e) TEM images of the resulting hybrid nanorod-plates. The samples for TEM characterization were detached from wafer.

soaked in a reaction solution of 4-MBA (350 μM), $HAuCl_4$ (1.7 mM) and L-ascorbic acid (4.1 mM). After a short reaction period (about 20 s), the wafer was retrieved, rinsed with ethanol to remove the reactants, and then immersed into a new reaction solution for growing Pd segments. As shown in Figure 4c,d, the resulting diblock NWs is not uniform in diameter along an individual NW, with an 8 nm width segment and a 4 nm width segment. As far as the width is concerned, the 8 nm segment is consistent with the Au NWs obtained from the same growth conditions and the 4 nm segment is consistent with the Pd NWs. However, the NW segments were too thin, so that distinguishing the top and bottom segments on the substrate is problematic using SEM.

The material composition of the bimetallic NWs was characterized by high-angle annular dark-field scanning TEM (HAADF-STEM) and energy dispersive X-ray spectrum (EDS) analyses (Figure 5b-d). Figure 5b shows a typical NW whose two segments can be easily distinguished given their large contrast difference. The thicker end is a Au-Pd alloy mainly composed of Au (85.7%), whereas the thinner end of the NW is only made of Pd (Figure 5c,d). Considering the two-step synthesis of the diblock NW, it is conceivable that a small amount of Pd atoms/ions may adsorb on the surface of the previously grown Au segment, given the likely ligand loss during the ethanol washing step. HRTEM confirmed that there was no obvious Pd layer on the Au segment (Figure 5a). Characterization of the Au-Pd interface showed that the Pd segment was grown epitaxially from the end of the Au segment

(Figure 5a), though the Au and Pd segments by themselves sometimes contained twin planes and polycrystalline domains (Figure 2d).

Similarly, Pd-Au diblock NWs were also synthesized by reversing the order of the growth. In other words, the Pd segment can be grown first, followed by the Au segment.[30]

Hybrid Nanorod-plate. To our great interest, when Au nanorods were used as seeds, hybrid nanorod-plate (Figure 1d) were obtained as a result of the line of active site between the Au nanorods and substrate. This is in contrast to the single-dot active site between a NP and the substrate. The product was detached from the substrate using sonication and the enriched sample was characterized by TEM (Figure 6b-e). The size and shape of the Au nanorods remained unchanged and the emerging Pd nanoplates only grew from one side of their surface. Some of the plates evolved to become multiple parallel Au NWs (d = 6 nm, Figure 6e), likely due to the random fluctuation of Au/ligand local concentrations during the growth. Some of the Pd nanoplates were obviously wedge-shaped (Figure 6c), suggesting persistently imbalanced growth rates.

This unique mode of nanocrystal growth can only be achieved *via* the Active Surface Growth. In contrast, in VLS growth the seeds are almost always molten, making it hard to create a line of growth sites for forming hybrid nanoplates. Likewise, it is difficult to fabricate hybrid nanoplates *via* templated growth[22,36] or defect-driven growth,[24,37-41] because of the lack of means for pre-arranging templates and defects at the nanoscale.

Conclusions

The growth of substrate-bound Pd and Ag NWs *via* the Active Surface Growth was found to be feasible but with narrow windows of reaction conditions. The unique characteristics of the Active Surface Growth mode are also manifested in Pd and Ag NWs, in addition to the previously studied Au NWs: the NWs can only grow from substrate-attached seeds, where the contact point is the active site of growth; the ligand is a critical factor unlike the VLS method; the diameter of NWs is independent of the seed size, but determined by the relative rates of ligand binding and metal deposition.

Most importantly, the growth mode, in addition of being facile and scalable, provides a versatile synthetic platform: (1) segmented hybrid NWs can be prepared *via* sequential growth; (2) the shape of active site can be pre-defined to control new types of hybrid nanostructures. These new synthetic capabilities are important advances towards sophisticated nanostructures.

Acknowledgements

The authors thank the A*Star (SERC 112-120-2011) and MOE (RG14/13) of Singapore for financial support.

Notes and references

[†]Division of Chemistry and Biological Chemistry, [‡]School of Materials Science and Engineering, and [§]School of Chemical and Biomedical Engineering, Nanyang Technological University, 637371, Singapore

*Correspondence should be addressed to: hongyuchen@ntu.edu.sg

Electronic Supplementary Information (ESI) available: Supporting TEM and SEM images of control experiments with different reaction conditions and another type of diblock nanowires. See DOI: 10.1039/b000000x/

1. D. Wang, Y. Li *Adv. Mater.* 2011, **23**, 1044.
2. X. Huang, N. Zheng *J. Am. Chem. Soc.* 2009, **131**, 4602.
3. J. Huang, Y. Zhu, M. Lin, Q. Wang, L. Zhao, Y. Yang, K. X. Yao, Y. Han *J. Am. Chem. Soc.* 2013, **135**, 8552.
4. Y.-C. Tsao, S. Rej, C.-Y. Chiu, M. H. Huang *J. Am. Chem. Soc.* 2013, **136**, 396.
5. T. J. Kempa, J. F. Cahoon, S.-K. Kim, R. W. Day, D. C. Bell, H.-G. Park, C. M. Lieber *Proc. Natl. Acad. Sci. USA* 2012, **109**, 1407.
6. B. Tian, X. Zheng, T. J. Kempa, Y. Fang, N. Yu, G. Yu, J. Huang, C. M. Lieber *Nature* 2007, **449**, 885.
7. L. Carbone, P. D. Cozzoli *Nano Today* 2010, **5**, 449.
8. Y. Pan, J. Gao, B. Zhang, X. Zhang, B. Xu *Langmuir* 2009, **26**, 4184.
9. D. Son, J. Lee, S. Qiao, R. Ghaffari, J. Kim, J. E. Lee, C. Song, S. J. Kim, D. J. Lee, S. W. Jun, S. Yang, M. Park, J. Shin, K. Do, M. Lee, K. Kang, C. S. Hwang, N. Lu, T. Hyeon, D.-H. Kim *Nat Nano* 2014, **9**, 397.
10. S. Sun *Adv. Mater.* 2006, **18**, 393.
11. Y. Feng, J. He, H. Wang, Y. Y. Tay, H. Sun, L. Zhu, H. Chen *J. Am. Chem. Soc.* 2012, **134**, 2004.
12. J. H. Lee, J. H. Wu, H. L. Liu, J. U. Cho, M. K. Cho, B. H. An, J. H. Min, S. J. Noh, Y. K. Kim *Angew. Chem.Int. Ed.* 2007, **46**, 3663.
13. S. R. Nicewarner-Peña, R. G. Freeman, B. D. Reiss, L. He, D. J. Peña, I. D. Walton, R. Cromer, C. D. Keating, M. J. Natan *Science* 2001, **294**, 137.
14. D. Seo, C. Il Yoo, J. Jung, H. Song *J. Am. Chem. Soc.* 2008, **130**, 2940.
15. J. Jung, D. Seo, G. Park, S. Ryu, H. Song *J. Phys. Chem. C* 2010, **114**, 12529.
16. M. R. Langille, J. Zhang, C. A. Mirkin *Angew. Chem. Int. Ed.* 2011, **50**, 3543.
17. X. Li, J. Lian, M. Lin, Y. Chan *J. Am. Chem. Soc.* 2010, **133**, 672.
18. S. K. Lim, S. Crawford, G. Haberfehlner, S. Gradečak *Nano Lett.* 2012, **13**, 331.
19. M. S. Gudiksen, L. J. Lauhon, J. Wang, D. C. Smith, C. M. Lieber *Nature* 2002, **415**, 617.
20. Y. Wu, R. Fan, P. Yang *Nano Lett.* 2002, **2**, 83.
21. S.-K. Kim, S. B. Lee *J. Mater. Chem.* 2009, **19**, 1381.
22. J. Wang *J. Mater. Chem.* 2008, **18**, 4017.
23. Y. Wang, J. He, c. Liu, W. H. Chong, H. Chen *Angew. Chem.Int. Ed.* 2014, DOI: 10.1002/anie.200.
24. Y. Sun, B. Mayers, T. Herricks, Y. Xia *Nano Lett.* 2003, **3**, 955.
25. D. J. Milliron, S. M. Hughes, Y. Cui, L. Manna, J. B. Li, L. W. Wang, A. P. Alivisatos *Nature* 2004, **430**, 190.
26. J. He, Y. Wang, Y. Feng, X. Qi, Z. Zeng, Q. Liu, W. S. Teo, C. L. Gan, H. Zhang, H. Chen *Acs Nano* 2013, **7**, 2733.
27. J. He, W. Ji, L. Yao, Y. Wang, B. Khezri, R. D. Webster, H. Chen *Adv. Mater.* 2014, **26**, 4151.
28. G. Frens *Nat. Pysics. Sci.* 1973, **241**, 20.
29. A. Gole, C. J. Murphy *Langmuir* 2007, **24**, 266.

30. , See Supporting Information for details.
31. K. K. Caswell, C. M. Bender, C. J. Murphy *Nano Lett.* 2003, **3**, 667.
32. X. M. Sun, Y. D. Li *Adv. Mater.* 2005, **17**, 2626.
33. D. Yu, V. W.-W. Yam *J. Phys. Chem. B* 2005, **109**, 5497.
34. A. Tao, F. Kim, C. Hess, J. Goldberger, R. He, Y. Sun, Y. Xia, P. Yang *Nano Lett.* 2003, **3**, 1229.
35. J.-Y. Lee, S. T. Connor, Y. Cui, P. Peumans *Nano Lett.* 2008, **8**, 689.
36. Q. Zhang, S. J. Liu, S. H. Yu *J. Mater. Chem.* 2009, **19**, 191.
37. J. Zhu, H. L. Peng, A. F. Marshall, D. M. Barnett, W. D. Nix, Y. Cui *Nat. Nanotechnol.* 2008, **3**, 477.
38. M. J. Bierman, Y. K. A. Lau, A. V. Kvit, A. L. Schmitt, S. Jin *Science* 2008, **320**, 1060.
39. S. A. Morin, M. J. Bierman, J. Tong, S. Jin *Science* 2010, **328**, 476.
40. S. Jin, M. J. Bierman, S. A. Morin *J. Phys. Chem. Lett.* 2010, **1**, 1472.
41. F. Meng, S. A. Morin, A. Forticaux, S. Jin *Acc. Chem. Res.* 2013, **46**, 1616.

Table of Contents

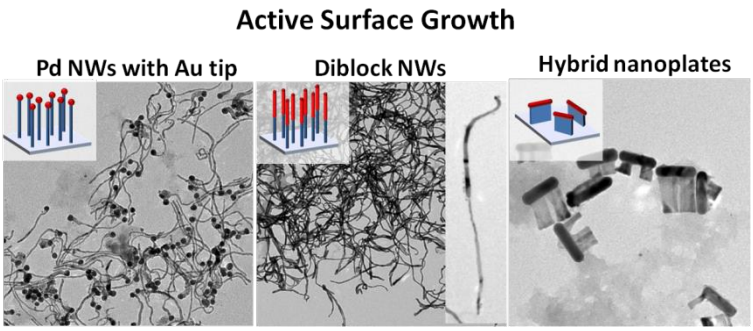

Active Surface Growth mechanism provides a versatile platform for the growth of substrate-bound Au-Pd diblock nanowires and hybrid nanorod-plate.